

Supporting Information

### Strain Effects on the Electronic and Transport Properties of TiO<sub>2</sub> Nanotubes

Xiaohui Yu<sup>1</sup>, Huilong Dong<sup>2</sup>, Lu Wang<sup>2</sup>, Youyong Li<sup>\*2</sup>

<sup>1</sup>Engineering Institute of Advanced Manufacturing and Modern Equipment Technology, Jiangsu University, Zhenjiang 212013, China

<sup>2</sup> Jiangsu Key Laboratory for Carbon-Based Functional Materials and Devices, Functional Nano & Soft Materials Laboratory (FUNSOM), Soochow University, Suzhou, Jiangsu, China, 215123

Emails: yyli@suda.edu.cn

The anatase phase TiO<sub>2</sub> belongs to the space group  $I4_1/amd$ . The monolayer TiO<sub>2</sub> can be viewed as cleaved from the {101} plane of anatase, which is characterized by TiO<sub>6</sub> octahedra. Therefore, tubular structures can be analogously constructed by conformal mapping of this two-dimensional (2D) triple layer of TiO<sub>2</sub> onto the surface of a cylinder, thus rolling up the sheets along specific directions in the 2D lattice. As for the carbon nanotubes this may be described in terms of the primitive 2D lattice vectors  $\vec{a}$  and  $\vec{b}$  and two integer indices:  $\vec{B} = n\vec{a} + m\vec{b}$ . In this way three classes of nanotubes can be distinguished:  $n=m$  “armchair” nanotube,  $n \neq 0, m=0$  “zigzag” nanotube, and  $n \neq m$  “chiral” nanotube. Furthermore, these nanotubes are composed of a triple layer of atoms with a finite “wall thickness” exhibiting certain “roughness” on the outer shell.

Our calculations were performed for “armchair”  $(n, n)$  and “zigzag”  $(n, 0)$  TiO<sub>2</sub> nanotubes as a function of  $n$  with diameter ( $D$ ) ranging between 8 and 27 Å, which correspond to indices  $(n, 0)$ - $(n, n)$  from  $(8, 0)$ - $(6, 6)$  to  $(16, 0)$ - $(14, 14)$ , respectively. The largest diameters are half as small as the experimentally observed TiO<sub>2</sub> nanotubes of medium diameters. The gap energy of “armchair”  $(n, n)$  TiO<sub>2</sub> nanotubes increases with increasing tube diameter, however, in contrast to “armchair”, the gap energy of “zigzag”  $(n, 0)$  TiO<sub>2</sub> nanotubes decreases with increasing tube diameter. But both show larger gap than the bulk material. Similar behavior has been reported

theoretically for “armchair” TiO<sub>2</sub> nanotubes. All the tubes are similar and consistent with the DOS of crystalline anatase. The valence band is composed by Ti 3d and O 2p states, the lower part of the conduction band is formed predominantly by Ti 3d states, see Figure S1.

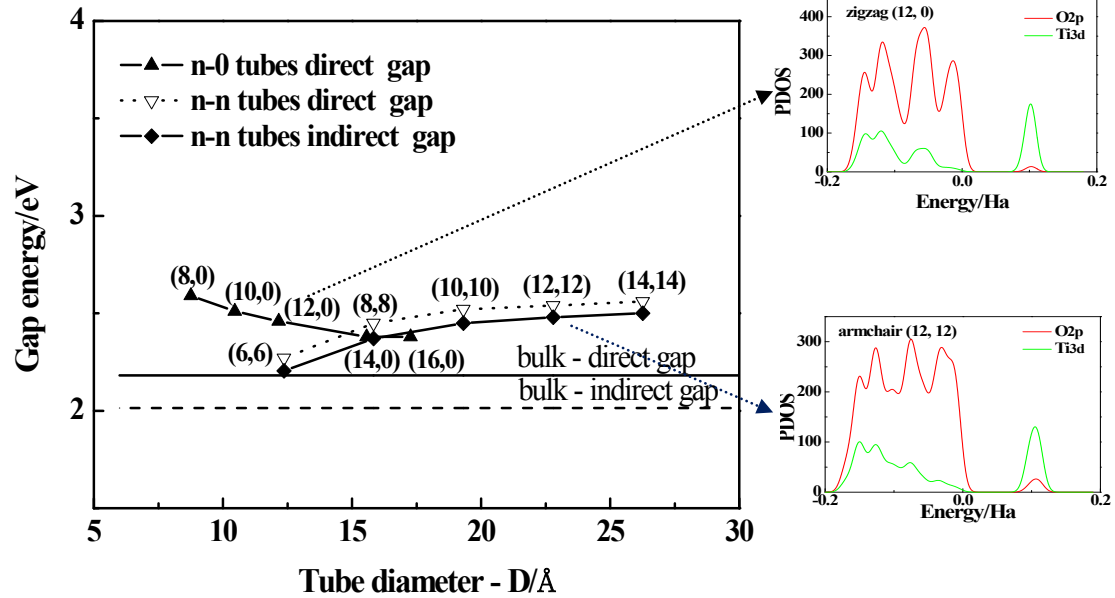


Figure S1. Calculated gap energies of TiO<sub>2</sub> nanotubes as a function of tube diameter in Å. The inserted images show density of states (DOS) of armchair (12, 12) TiO<sub>2</sub> nanotube and zigzag (12, 0) TiO<sub>2</sub> nanotube.

To understand the stability of TiO<sub>2</sub> nanotubes via isotropic strain, we calculated the total energies variation of TiO<sub>2</sub> nanotubes as a function of isotropic strain (see Figure S2). The total energies variation ( $\Delta E$ ) for the larger TiO<sub>2</sub> tubes (armchair (12, 12) and zigzag (12, 0)) is lower than that of the smaller one (armchair (8, 8) and zigzag (8, 0)) with  $\epsilon=0\%$  strain. This result is not surprising, since the rolling of a monolayer into a smaller tube cause more strain energy than a larger one. The  $\Delta E$  for zigzag (n, 0) TiO<sub>2</sub> nanotubes is slightly more favorable than for with  $\epsilon=0\%$  strain.

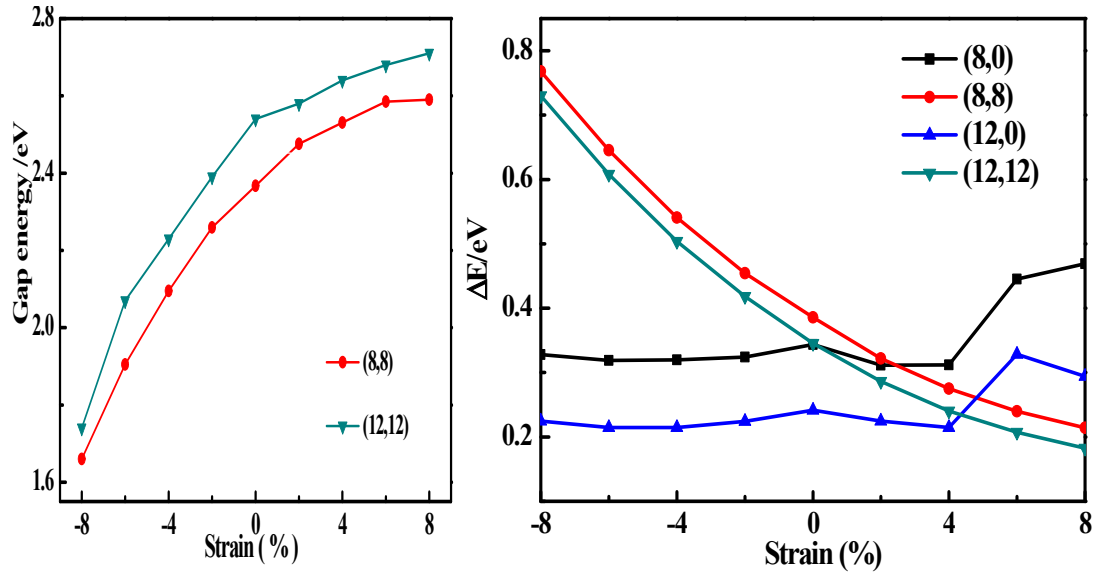


Figure S2. Calculated gap energies (left) and total energies variation ( $\Delta E$ ) (right) of  $\text{TiO}_2$  nanotubes versus isotropic strain.

The DFT setting for VASP:

Projector-augmented-wave (PAW) potentials<sup>1</sup> were used to take into account the electron–ion interactions, and the electron exchange correlation interactions were treated using generalized gradient approximation (GGA)<sup>2</sup> in the scheme of Perdew–Burke–Ernzerhof. An energy cut-off of 600 eV was used for the plane-wave expansion. The strain (compressive or tensile) was applied on the axial direction by fixing the axial vectors ( $c/z$ ) at a fixed value to construct the strained structure. In the radial directions ( $a/x$  and  $b/y$ ), a vacuum space of 15 Å was kept to avoid mirror interactions. Atomic relaxation was performed until the change of total energy was less than 0.01 meV and all the forces on each atom were smaller than 0.02 eV/Å. For nanotubes, the primitive cell contains 72 atoms for (12, 0) and (12, 12) nanotubes, respectively. A  $k$ -point sampling of  $1 \times 1 \times 20$  was used to calculate density of states (DOS).

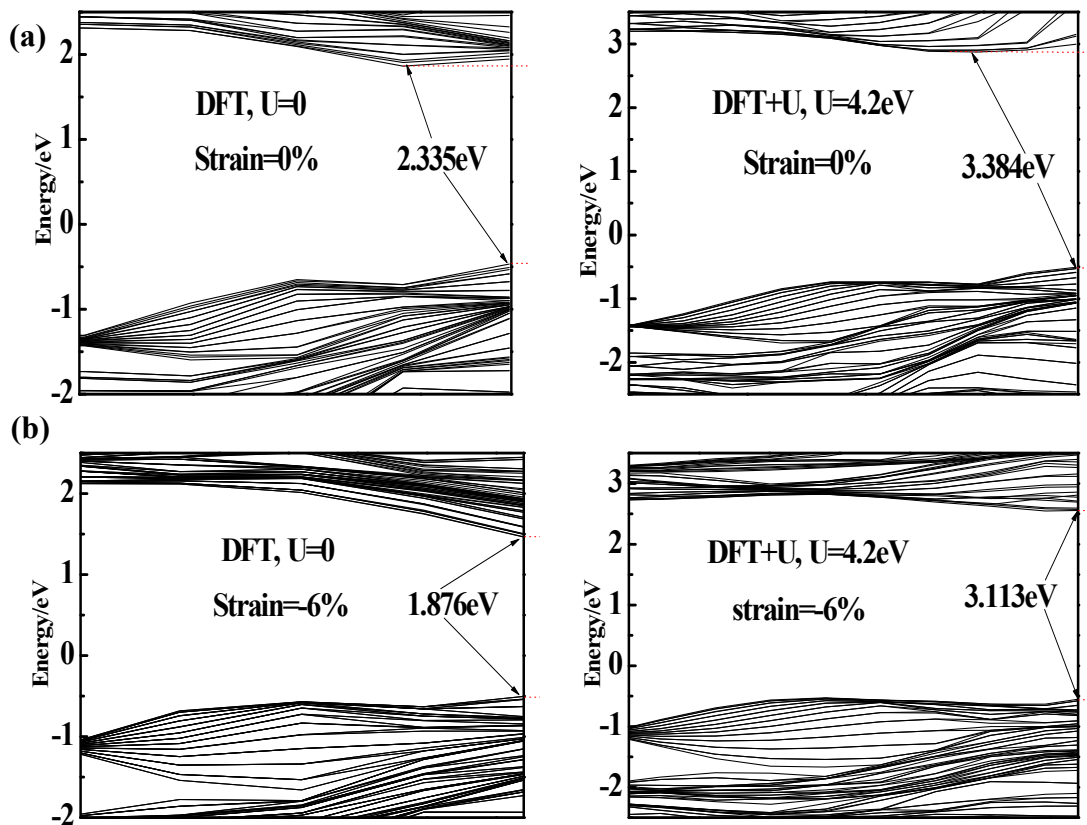


Figure S3 Electronic band structures for TiO<sub>2</sub> nanotubes. (a) The (12, 12) TiO<sub>2</sub> nanotubes at strain  $\epsilon=0\%$  with (or without) DFT+U method, (b) The (12, 12) TiO<sub>2</sub> nanotubes at strain  $\epsilon=-6\%$  (compressive strain) with (or without) DFT+U method. The DFT+U improve the calculated band gap, and the trend predicted by DFT+U is consistent with that by GGA.

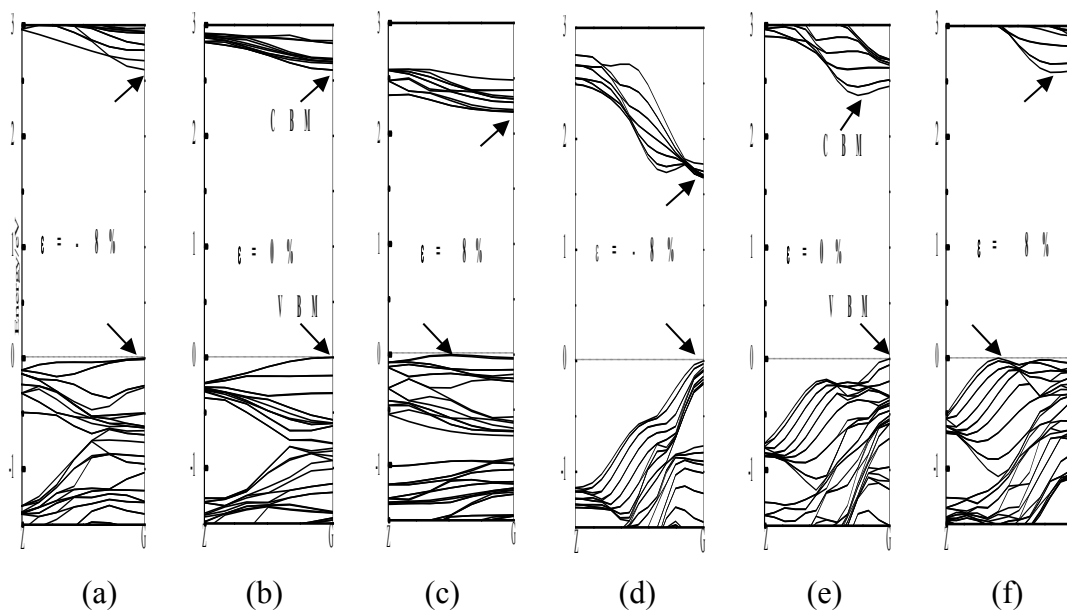


Figure S4. Electronic structure of (a)-(c) (8, 0) and (d)-(f) (8, 8) TiO<sub>2</sub> nanotubes at strain  $\varepsilon=-8\%$ ,  $0\%$ , and  $8\%$ , respectively. The position of conduction band minimum (CBM) and valence band maximum (VBM) are indicated by the arrows. The dashed line denotes the Fermi level.

### References

- (1) Blochl, P. E. *Phys. Rev. B* **1994**, 50, 17953.
- (2) Perdew, J. P.; Chevary, J. A.; Vosko, S. H.; Jackson, K. A.; Pederson, M. R.; Singh, D. J.; Fiolhais, C. *Phys. Rev. B* **1992**, 46, 6671.